

Investigation of phase transition in ferroelectric $\text{Pb}_{0.70}\text{Sr}_{0.30}\text{TiO}_3$ thin films

F. M. Pontes, S. H. Leal, E. R. Leite, E. Longo, P. S. Pizani, A. J. Chiquito, and J. A. Varela

Citation: *Journal of Applied Physics* **96**, 1192 (2004); doi: 10.1063/1.1758314

View online: <http://dx.doi.org/10.1063/1.1758314>

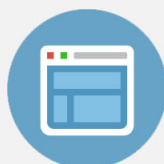
View Table of Contents: <http://scitation.aip.org/content/aip/journal/jap/96/2?ver=pdfcov>

Published by the [AIP Publishing](#)



Re-register for Table of Content Alerts

Create a profile.



Sign up today!



Investigation of phase transition in ferroelectric $\text{Pb}_{0.70}\text{Sr}_{0.30}\text{TiO}_3$ thin films

F. M. Pontes, S. H. Leal, E. R. Leite, and E. Longo^{a)}

Department of Chemistry, LIEC-CMDMC, Universidade Federal de São Carlos Via Washington Luiz, km 235, CP-676, CEP-13565-905, São Carlos, São Paulo, Brazil

P. S. Pizani and A. J. Chiquito

Department of Physics, Universidade Federal de São Carlos Via Washington Luiz, km 235, CEP-13565-905, São Carlos, São Paulo, Brazil

J. A. Varela

Institute of Chemistry, UNESP, Araraquara, São Paulo, Brazil

(Received 26 September 2003; accepted 10 April 2004)

We have carried out dielectric and Raman spectroscopy studies at the 298–623 K temperature range in polycrystalline $\text{Pb}_{0.70}\text{Sr}_{0.30}\text{TiO}_3$ thin films grown by a soft chemical method. The diffuse phase-transition behavior of the thin films was observed by means of the dielectric constant versus temperature curves, which show a broad peak. Such behavior was confirmed later by Raman spectroscopy measurements up to 823 K, indicating that a diffuselike phase transition takes place at around 548–573 K. The damping factor of the $E(1TO)$ soft mode was calculated using the damped simple harmonic oscillator model. On the other hand, Raman modes persist above the tetragonal to cubic phase transition temperature although all optical modes should be Raman inactive. The origin of these modes was interpreted in terms of a breakdown of the microscopic local cubic symmetry by chemical disorder. The lack of a well-defined transition temperature and the presence of broad bands at some temperature interval above the ferroelectric-paraelectric phase-transition temperature suggested a diffuse nature of the phase transition. This result corroborates the dielectric constant versus temperature data, which showed a broad ferroelectric phase transition in this thin film.

© 2004 American Institute of Physics. [DOI: 10.1063/1.1758314]

I. INTRODUCTION

Recently, many ferroelectric thin films such as $(\text{Pb,Ca})\text{TiO}_3$, $\text{Ba}(\text{Zr,Ti})\text{O}_3$, PbTiO_3 , and $(\text{Pb,Sr})\text{TiO}_3$ have been actively investigated for application in memory integrated circuits.^{1–3} Lead titanate (PbTiO_3) based materials are used in a wide range of electronic devices, e.g., transducers, infrared detectors, ferroelectric memories, etc.^{4,5} In addition, thin films of solid solutions of PbTiO_3 with other perovskite compounds exhibit an enhancement in various interesting properties and are, thus, feasible to be used in several devices. With the addition of strontium to PbTiO_3 , the phase-transition temperature decreases with the increasing strontium concentration. It is also interesting to note that many ferroelectric materials, such as thin films or bulk material, exhibit phase-transition relaxor behavior characteristics that appear mainly in oxygen octahedron families, i.e., in the perovskite-type structure and in the tungsten-bronze-type structure (TKWB).^{6,7} Among the perovskite-type structure compounds, complex lead-based structures with two different cations in the same crystallographic site are particularly concerned. Well-known examples are lead magnesium niobate (PMN), lead zinc niobate (PZN), and their solid solutions with lead titanate (PT), which are the most widely studied relaxor materials.^{8–11} However, some lead-free compounds were also recently found to present a relaxor

behavior. In $\text{BaZr}_x\text{Ti}_{1-x}\text{O}_3$ compounds, the relaxor behavior depends on the zirconium content.¹² One of the characteristics of the relaxor ferroelectrics is the strong influence of the frequency f of the electric field on the curves $\epsilon-T$, i.e., when f increases, ϵ decreases, and the ϵ maximum temperature increases. In addition, the relaxor characteristics of PT with higher La concentration are reported in the literature.¹³ The typical phase-transition phenomenon in materials, either classical or relaxor ferroelectrics, has been extensively investigated in the literature by electrical measurements or Raman spectroscopy. Naik *et al.*¹⁴ reported a study on a $\text{Pb}_{0.4}\text{Sr}_{0.6}\text{TiO}_3$ thin film, in which the dielectric permittivity versus temperature data showed a broad peak at room temperature, indicating a rather diffuse phase transition. Studies of Ito *et al.*¹⁵ on bulk $\text{Pb}_{1-x}\text{Ba}_x\text{TiO}_3$ solid solutions showed a diffuse ferroelectric to paraelectric transition, associated with a broad $\epsilon(T)$ anomaly over a wide temperature range. On the other hand, Tenne *et al.*¹⁶ studied vibrational properties of $\text{Ba}_{0.5}\text{Sr}_{0.5}\text{TiO}_3$ thin films prepared by pulsed laser deposition and they observed that the temperature dependence of the Raman spectra indicates a broad ferroelectric phase transition in the thin films. Dobal *et al.*¹⁷ studied, by Raman scattering and dielectric constant as a function of the temperature, the antiferroelectric phase transition in PbZrO_3 thin films. These PbZrO_3 thin films exhibited a clear temperature-dependent phase transition from the antiferroelectric to the paraelectric state, through a ferroelectric

^{a)}Electronic mail: liec@power.ufscar.br

phase. Gakh *et al.*¹⁸ reported the phase transition of $\text{Pb}_{1-x}\text{Ca}_x\text{TiO}_3$ thin films. The $x=0.15$ thin film was found to undergo a tetragonal-to-cubic phase transition at about 370 °C. Although many authors have investigated $\text{Pb}_{1-x}\text{Sr}_x\text{TiO}_3$ (PST) thin films and ceramic solid solutions, no systematic study of the temperature dependence of dielectric constant and Raman spectra in the study of phase transition of polycrystalline $\text{Pb}_{0.7}\text{Sr}_{0.3}\text{TiO}_3$ thin films was discussed in the literature.

In this paper, we report an investigation on the temperature dependence of the dielectric permittivity and Raman spectra of $\text{Pb}_{0.7}\text{Sr}_{0.3}\text{TiO}_3$ thin films prepared by a soft chemical method on Pt-coated silicon substrate.

II. EXPERIMENT

The $\text{Pb}_{0.7}\text{Sr}_{0.3}\text{TiO}_3$ (PST30) thin films studied in the present work were derived from a soft chemical processing. Details of the preparation method can be found in the literature.¹⁹ The polymeric precursor solution was spin-coated on substrates [Pt (140 nm)/Ti (10 nm)/ SiO_2 (1000 nm)/Si] by a commercial spinner operating at 6000 rpm for 30 s (spin-coater KW-4B, Chemat Technology), via a syringe filter to avoid particulate contamination. After the spinning, the films were kept in ambient air at 150 °C on a hot plate for 20 min to remove residual solvents. A two-stage heat treatment was carried out: initial heating at 400 °C for 4 h at a heating rate of 1 °C/min to pyrolyze the organic materials and finally followed by heating at 600 °C for 2 h for crystallization.

The temperature-dependent dielectric constant of the thin film was studied in metal-ferroelectric-metal configuration and the film was characterized using a Keithley 3330 (LCR) meter at the temperature range of 298–653 K. The capacitance–voltage (C – V) curves were measured using an HP4194A impedance/gain phase analyzer at the temperature range of 298–573 K. The leakage current–voltage (I – V) characteristic was determined with a voltage source measuring unit (Keithley 237). For these measurements, circular Au electrodes of $3.15 \times 10^{-2} \text{ mm}^2$ area were deposited by evaporation process on the surfaces of the heat-treated films as top electrodes, through a shadow mask.

Particularly, the ferroelectric materials present a close relationship between ferroelectricity and lattice dynamics. Therefore, Raman spectroscopy has been a valuable technique to characterize phase transitions in these materials, because the structural changes associated with the ferroelectric to paraelectric phase transition usually present a large influence on the Raman spectra. The Raman measurements were performed using a T-6400 Jobin-Yvon triple-monochromator, coupled to a charge-coupled device (CCD) detector. An optical microscope with a 50 \times objective was used to focus the 514.5 nm line of Coherent Innova 90 argon laser into the sample. The power was kept at 22 mW. A TMS 93 oven from Linkam Scientific Instruments Ltd. was used under the microscope for the measurements at the 298–823 K temperature range.

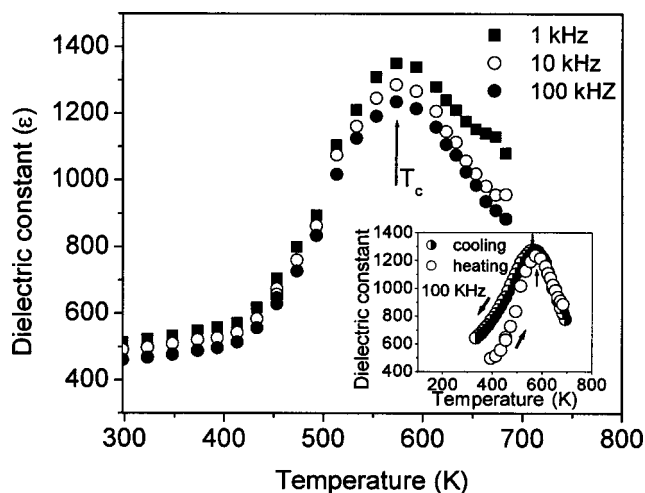


FIG. 1. Variation of dielectric constant with temperature of $\text{Pb}_{0.7}\text{Sr}_{0.3}\text{TiO}_3$ thin film at different frequencies. The inset shows the variation of the dielectric constant of $\text{Pb}_{0.7}\text{Sr}_{0.3}\text{TiO}_3$ thin film as a function of temperature, during heating and cooling cycles at 100 kHz.

III. RESULTS AND DISCUSSION

The temperature and frequency variations of the dielectric constant for the PST30 thin film are shown in Fig. 1. We may notice that T_C , the temperature corresponding to the peak of the dielectric constant versus temperature is broader than that corresponding peak of compositions, close to PST30 in the bulk form. However, measurements at different frequencies do not show any peak shift. For a normal ferroelectric, in the vicinity of the transition temperature, the dielectric stiffness ($1/\epsilon$) follows the well-known Curie-Weiss law:²⁰

$$1/\epsilon = (T - T_0)/C, \quad (1)$$

where C is Curie-Weiss constant and T_0 is the Curie-Weiss temperature.

In addition, the order of the ferroelectric to paraelectric phase transition can be determined from the temperature de-

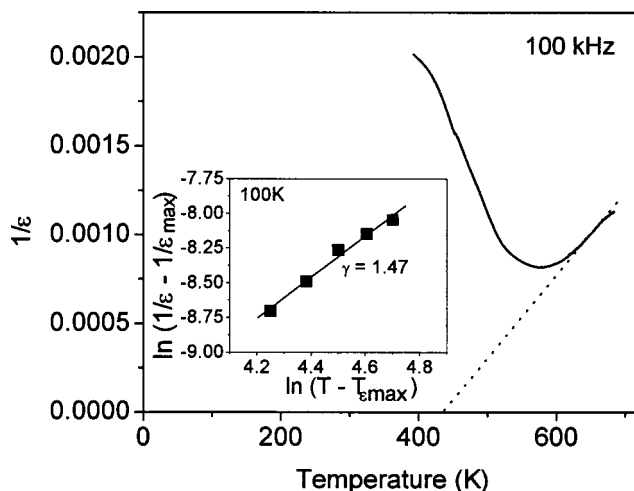


FIG. 2. The inverse of the dielectric constant, ($1/\epsilon$), as a function of temperature for the $\text{Pb}_{0.7}\text{Sr}_{0.3}\text{TiO}_3$ thin film. The inset shows $\ln(1/\epsilon - 1/\epsilon_{\text{max}})$ as a function of $\ln(T - T_{\epsilon_{\text{max}}})$.

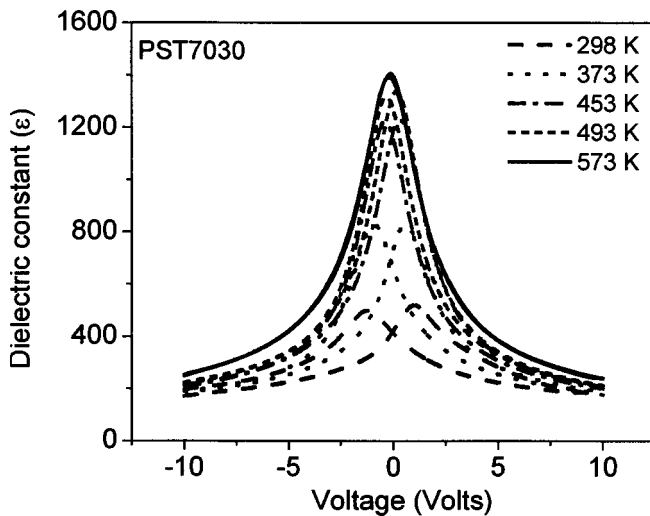


FIG. 3. Dielectric constant-voltage characteristics of the $\text{Pb}_{0.70}\text{Sr}_{0.30}\text{TiO}_3$ thin film at different temperatures at 100 kHz.

pendence of the dielectric constant inverse ($1/\epsilon$). When T_0 is smaller than T_C , we observe a first-order transition; on the other hand, when $T_0 = T_C$, a second-order transition is observed.²¹

Figure 2 shows the temperature behavior of the inverse of the dielectric constant at 100 kHz for the PST30 thin film. The parameters C and T_0 were fitted at a narrow temperature range near T_C . From these data, the ferroelectric to paraelectric phase transition temperature T_C and the Curie-Weiss temperature T_0 can be obtained directly. The fitting parameters are $C = 4.58 \times 10^6$ K and $T_0 = 430$ K. The fact that the Curie-Weiss temperature ($T_0 = 430$ K) is lower than the transition temperature ($T_C = 573$ K) is expected from the first-order phase transition between the paraelectric and ferroelectric phases. Furthermore, the inset in Fig. 1 shows that the ferroelectric phase of PST30 transforms into the paraelectric phase at 573 K during the heating cycle. A thermal hysteresis of about 10 K in the transition temperatures, obtained using heating and cooling cycles can be observed. This behavior is indicative of a first-order phase transition. In the literature, for a diffuse transition, the following empirical modification of the Curie-Weiss Law was proposed to describe the diffuseness of the phase transition as:²²

$$1/\epsilon - 1/\epsilon_m = (T - T_{\epsilon \max})^\gamma / C^*, \quad (2)$$

where γ is the critical exponent, which is a measure of the degree of diffuseness of the transition, and C^* is a Curie-Weiss-like constant. For a sharp transition, $\gamma = 1$ and for a diffuse transition it lies in the range $1 < \gamma \leq 2$.²³ We obtained the parameter $\gamma = 1.47$ by fitting the experimental data (the fitting curve is shown in the inset of Fig. 2). From these data, we may note that there is some diffuse character, but measurements at different frequencies showed that the peak temperature is not seriously affected by the change in frequency (see Fig. 1). Such a behavior indicates that the transition is relatively diffuse, but that the ferroelectric phase is not relaxor in the PST30 thin film. The observed broad curve behavior displayed by the thin film, unlike the bulk behavior, suggests that the smaller grain size of thin film (about 120

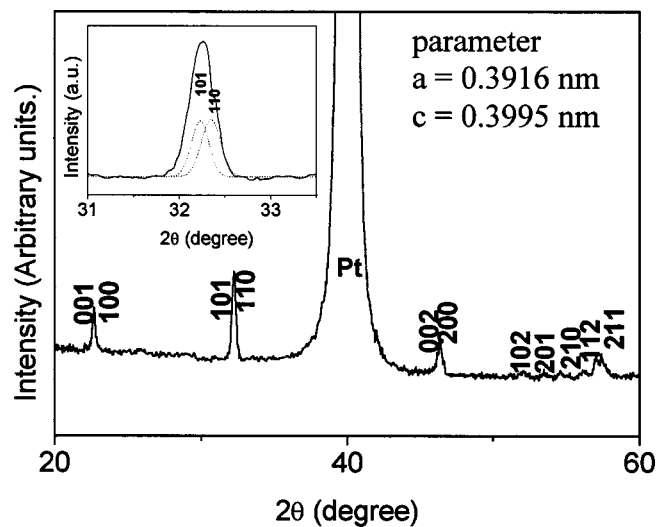


FIG. 4. The x-ray diffraction pattern of $\text{Pb}_{0.70}\text{Sr}_{0.30}\text{TiO}_3$ thin film prepared on platinum-coated silicon substrate. The inset shows a selected 2θ region of the (101)/(110) diffraction peak.

nm) relative to bulk causes some type of strain between the grain boundary interfaces, which is generally responsible for the observed transition. Similar behavior was observed by Subrahmanyam and Goo for the $(\text{Pb}_x\text{Sr}_{1-x})\text{TiO}_3$ system.²⁴ Pokharel and Pandey reported values of γ in the range of 1.25–1.50 for the diffuse behavior of the $(\text{Pb}_{1-x}\text{Ba}_x)\text{ZrO}_3$ system.²⁵ In addition, Ganesh and Goo reported values of γ in the range of 1.20–1.34 for the diffuse behavior of the paraelectric-ferroelectric transition region for the $(\text{Pb}_{1-x}\text{Ca}_x)\text{TiO}_3$ system.²⁶

Figure 3 shows the dielectric constant-voltage ($\epsilon-V$) curves of the PST30 thin film deposited on Pt/Ti/SiO₂/Si substrate. The $\epsilon-V$ curves were obtained at different temperatures at the frequency of 100 kHz with an oscillation amplitude of 50 mV. The capacitance of the film showed a

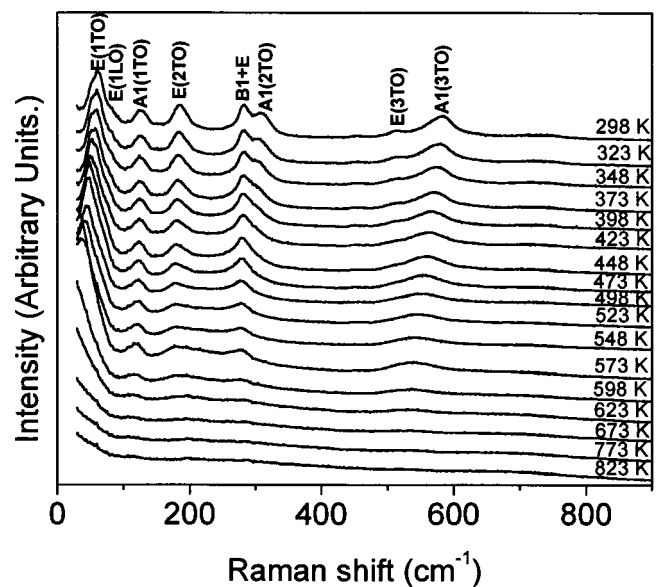


FIG. 5. Raman spectra of $\text{Pb}_{0.70}\text{Sr}_{0.30}\text{TiO}_3$ thin film above and below the transition temperature.

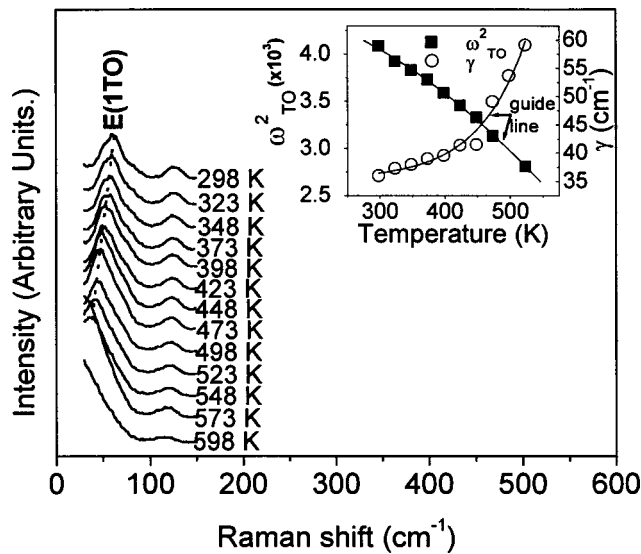


FIG. 6. Low-frequency Raman spectra of $\text{Pb}_{0.70}\text{Sr}_{0.30}\text{TiO}_3$ thin film as a function of temperature. The inset shows the temperature dependence of the $E(1TO)$ mode peak frequency (ω_{TO}^2) and damping factor γ as deduced from Eq. (3).

strong dependence on the applied voltage. At 298 K, the $\epsilon-V$ curve showed two broad peaks and the curve was symmetric about the zero-bias axis and a hysteresis behavior was observed. Increasing the temperature, the butterfly-type shape of the curves was decreased: the separation between the $\epsilon-V$ curves of the positive and negative bias was decreased and, at about 573 K, the $\epsilon-V$ curves showed the absence of splitting (butterfly-type) for the decreasing and the increasing voltage for both polarities. This fact indicates that the temperature 573 K corresponds to the ferroelectric-paraelectric phase transition.

The crystal structure of the thin film was examined by a Rigaku x-ray diffractometer with $\text{Cu K}\alpha$ radiation. Figure 4 shows that the thin film was well crystallized without any unexpected phases.

In order to study the phase transition by Raman spectroscopy, the spectra were obtained at different temperatures and the results are shown in Fig. 5. The room temperature Raman spectrum is in agreement with those reported in the literature, showing all Raman active optical modes.¹⁹ According to the Raman selection rules, all optical modes become Raman inactive above the transition temperature. With the increase of the temperature a decrease in the intensity and a broadening of the Raman peaks can be observed. There are, however, some important features in some Raman peaks, which disappear completely at a certain critical temperature, which corresponds to the ferroelectric to paraelectric phase-transition temperature. Conversely, some peaks persist even at temperatures above the transition. Figure 6 shows the temperature dependence of the $E(1TO)$ lowest frequency Raman mode, whose frequency goes to zero at about 570 K, as shown in Fig. 5. This typical soft mode behavior is responsible for the ferroelectric to paraelectric phase transition. Furthermore, important information can be obtained by a detailed examination to the temperature dependence of the line shape of the soft mode, in the light of the damped classical

harmonic oscillator model, to properly determine the damping factor γ as a function of temperature. According to following equation,^{27,28}

$$I(\omega) \propto \frac{KTP_s \epsilon'(\omega) \gamma \omega_{TO}^2}{(\omega_{TO}^2 - \omega^2)^2 + \gamma^2 \omega^2}, \quad (3)$$

where P_s is the spontaneous polarization and $\epsilon'(\omega)$ is the real part of the dielectric constant. A computer fitting of Eq. (3) of the line shape was carried out and the damping factors γ were obtained for the soft mode $E(1TO)$, as a function of temperature, as displayed in Fig. 6 (inset). Concerning the damping factor γ , a marked increase is observed near the phase-transition temperature. Such an increase of the damping is observed in a wide range of solid solution perovskite ferroelectrics for the soft mode $E(1TO)$. A similar observation was reported by Yu *et al.*²⁹ in $\text{SrBi}_2\text{Ta}_2\text{O}_9$ nanoparticles and in lead titanate thin films on sapphire, reported by Dobal *et al.*³⁰ A different value for transition-phase temperature was estimated from temperature dependence of the damping factor using the damped classical oscillator model. The transition temperature determined was at about 523 K, smaller than the one obtained by electrical measurements. Above this temperature, as can be seen in Figs. 5 and 6, the temperature dependence of the damping factor of the $E(1TO)$ mode has not been experimentally well fitting, so it is impossible to fit the data over the whole temperature range. Fu *et al.*³¹ reported phonon mode behaviors similar to PbTiO_3 thin films deposited on Pt/Si substrates where the transition-phase temperature was estimated by damping factor.

In addition, the temperature dependence of the square of the soft mode frequency is also shown in Fig. 6(inset). However, we can see that in the case of PST30 thin film, the persistence of phonon modes well beyond the transition temperature is owed to a short-range structural disorder in the paraelectric cubic phase. This disorder destroys the perfect cubic local symmetry and thus allows Raman activity in the paraelectric phase. Due to the persistence of the broad bands at temperature intervals above the phase transition, we believe that the phase transition in PST30 thin films is of diffuse nature. Similar observation was reported in thin films by Naik *et al.*³² for $(\text{Pb,Sr})\text{TiO}_3$ and in bulk $(\text{Pb,Lu})\text{TiO}_3$.³³ The disappearance of the 62 cm^{-1} soft modes at about 548–573 K indicates that the transformation from the ferroelectric to the paraelectric phase occurs at this $(\text{Pb,Lu})\text{TiO}_3$.³³ The disappearance of the 62 cm^{-1} soft modes at about 548–573 K indicates that the transformation from the ferroelectric to the paraelectric phase occurs at this temperature range, which is consistent with the Curie temperature determined by the electrical characterization.

IV. CONCLUSIONS

In summary, Raman spectroscopy and dielectric properties were used to examine the ferroelectric phase transition in a $\text{Pb}_{0.70}\text{Sr}_{0.30}\text{TiO}_3$ thin film as grown by a soft chemical method. We found that a diffuse phase transformation was observed in the prepared thin film, as the dielectric constant as a function of temperature curves shows a broad peak. It is revealed that the ferroelectric phase transition is not a

relaxor-type transition, once the phase-transition temperature was independent of the frequency (classical ferroelectric). Raman spectroscopy results confirm the existence of a diffuse-type phase transition around 548–573 K. This transition type is accompanied by the gradual disappearance of the overdamped $E(1TO)$ soft mode. We also found that broad Raman bands are seen to persist above the transition temperature. This is attributed to the breakdown of selection rules due to the presence of a microscopic local structural disorder in the paraelectric phase. Both dielectric and Raman scattering studies showed a diffuse nature of the phase transition.

ACKNOWLEDGMENTS

The authors gratefully acknowledge the financial support of the Brazilian financing agencies FAPESP/CEPID and CNPq/PRONEX.

- ¹C. S. His, C. Y. Chen, N. C. Wu, and M. C. Wang, *J. Appl. Phys.* **94**, 598 (2003).
- ²H. Ota, H. Fujino, S. Migita, S.-B. Xiong, and S. Sakai, *J. Appl. Phys.* **89**, 8153 (2001).
- ³K. T. Kim and C. I. Kim, *Thin Solid Films* **420–421**, 544 (2002).
- ⁴D. Fu, T. Ogawa, H. Suzuki, and K. Ishikawa, *Appl. Phys. Lett.* **77**, 1532 (2000).
- ⁵V. R. Palkar, S. C. Purandare, P. Ayyub, and R. Pinto, *J. Appl. Phys.* **87**, 462 (2000).
- ⁶C. Elissalde and J. Ravez, *J. Mater. Chem.* **11**, 1957 (2001).
- ⁷J. Ravez, *C. R. Acad. Sci., Ser. IIC; China* **3**, 267 (2000).
- ⁸X. Gao, J. Xue, T. Yu, Z. Shen, and J. Wang, *J. Am. Ceram. Soc.* **85**, 833 (2002).
- ⁹S. F. Liu, S. E. Park, T. R. Shrout, and L. E. Cross, *J. Appl. Phys.* **85**, 2810 (1999).
- ¹⁰J. H. Park, K. H. Yoon, D. H. Kang, and J. Park, *Mater. Chem. Phys.* **79**, 151 (2003).
- ¹¹A. L. Kholkin, E. K. Akdogan, A. Safari, P.-F. Chauvy, and N. Setter, *J. Appl. Phys.* **89**, 8066 (2001).
- ¹²P. S. Dobal, A. Dixit, R. S. Katiyar, Z. Yu, R. Guo, and A. S. Bhalla, *J. Appl. Phys.* **89**, 8085 (2001).
- ¹³T. Y. Kim, H. M. Jang, and S. M. Cho, *J. Appl. Phys.* **91**, 336 (2002).
- ¹⁴V. M. Naik, D. Haddad, R. Naik, J. Mantese, N. W. Schubring, A. L. Micheli, and G. W. Auner, *J. Appl. Phys.* **93**, 1731 (2003).
- ¹⁵Y. Ito, S. Shimada, J. I. Takahashi, and M. Inagaki, *J. Mater. Chem.* **7**, 781 (1997).
- ¹⁶D. A. Tenne, A. M. Clark, A. R. James, K. Chen, and X. X. Xi, *Appl. Phys. Lett.* **79**, 3836 (2001).
- ¹⁷P. S. Dobal, R. S. Katiyar, S. S. N. Bharadwaja, and S. B. Krupanidhi, *Appl. Phys. Lett.* **78**, 1730 (2001).
- ¹⁸S. G. Gakh, T. P. Myasnikova, O. A. Bunina, T. A. Yusman, and I. A. Cherepkova, *Inorg. Mater.* **33**, 416 (1997).
- ¹⁹F. M. Pontes *et al.*, *J. Mater. Res.* **18**, 659 (2003).
- ²⁰M. E. Lines and A. M. Glass, *Principles and Applications of Ferroelectrics and Related Materials* (Clarendon, Oxford, 1977).
- ²¹J. Ravez, C. Brouster, and A. Simon, *J. Mater. Chem.* **9**, 1609 (1999).
- ²²K. Uchini and S. Namura, *Ferroelectr., Lett. Sect.* **34**, 2551 (1982).
- ²³B. P. Pokharel and D. Pandey, *J. Appl. Phys.* **88**, 5364 (2000).
- ²⁴S. Subrahmanyam and E. Goo, *Acta Mater.* **46**, 817 (1998).
- ²⁵B. P. Pokharel and D. Pandey, *J. Appl. Phys.* **88**, 5364 (2000).
- ²⁶R. Ganesh and E. Goo, *J. Am. Ceram. Soc.* **89**, 653 (1997).
- ²⁷G. Burns and B. A. Scott, *Phys. Rev. Lett.* **25**, 167 (1970).
- ²⁸G. Burns and B. A. Scott, *Phys. Rev. B* **7**, 3088 (1973).
- ²⁹T. Yu, Z. X. Shen, W. S. Toh, J. M. Xue, and J. Wang, *J. Appl. Phys.* **94**, 618 (2003).
- ³⁰P. S. Dobal, S. Bhaskar, S. B. Majumder, and R. S. Katiyar, *J. Appl. Phys.* **86**, 828 (1999).
- ³¹D. S. Fu, H. Iwazaki, H. Suzuki, and K. Ishikawa, *J. Phys.: Condens. Matter* **12**, 399 (2000).
- ³²R. Naik *et al.*, *Phys. Rev. B* **61**, 11 367 (2000).
- ³³E. C. S. Tavares, P. S. Pizani, and J. A. Eiras, *Appl. Phys. Lett.* **72**, 897 (1998).